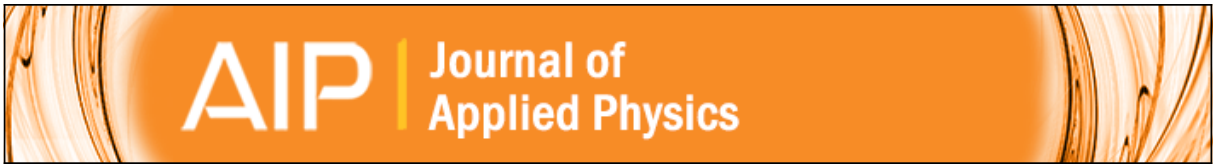

Dynamic FE simulation of μMAG standard problem No. 2 (invited)

B. Streibl, T. Schrefl, and J. Fidler

Citation: Journal of Applied Physics **85**, 5819 (1999); doi: 10.1063/1.369930
View online: http://dx.doi.org/10.1063/1.369930
View Table of Contents: http://scitation.aip.org/content/aip/journal/jap/85/8?ver=pdfcov
Published by the AIP Publishing

Articles you may be interested in

Enhanced M r and (B H) m a x in anisotropic R 2 Fe 14 B/α Fe composite magnets via intergranular magnetostatic coupling
J. Appl. Phys. **99**, 08B506 (2006); 10.1063/1.2162818

Investigation of hard magnetic properties of nanocomposite Fe-Pt magnets by micromagnetic simulation
J. Appl. Phys. **96**, 3921 (2004); 10.1063/1.1792812

Nonuniform magnetic structure in Nd 2 Fe 14 B/Fe 3 B nanocomposite materials
J. Appl. Phys. **93**, 8119 (2003); 10.1063/1.1537702

Behavior of μMAG standard problem No. 2 in the small particle limit
J. Appl. Phys. **87**, 5520 (2000); 10.1063/1.373391

Dynamic micromagnetics of nanocomposite NdFeB magnets
J. Appl. Phys. **81**, 5567 (1997); 10.1063/1.364663

[This article is copyrighted as indicated in the article. Reuse of AIP content is subject to the terms at: http://scitation.aip.org/termsconditions. Downloaded to] IP: 142.150.190.39 On: Mon, 22 Dec 2014 09:55:03

Dynamic FE simulation of μMAG standard problem No. 2 (invited)

B. Streibl, T. Schrefl,[a] and J. Fidler
Institute of Applied Physics, Technischen Universitat Vienna, Wiedner Hauptstrasse 8, A-1040 Vienna, Austria

μMAG standard problem No. 2 was studied using a three-dimensional finite element simulation based on the solution of the Gilbert equation. Asymptotic boundary conditions were imposed in order to compute the demagnetizing fields and a Gilbert-damping parameter (α=1.0) was used to drive the system towards equilibrium. The coercivities observed for the thin elongated platelet on which standard problem No. 2 is based show a slight dependence on its size. The width of the particle was varied from 1 to 30 times the exchange length while keeping the aspect ratio of 5:1:0.1 unchanged. An external field is applied parallel to the [111] direction, giving values of the coercive field ranging from -0.056 to -0.04 in units of the saturation magnetization M_s. With the external field applied parallel to the long axis of the particle a strong dependence of the coercivity on its size is found which can be attributed to different reversal mechanisms. © *1999 American Institute of Physics.* [S0021-8979(99)28308-9]

I. INTRODUCTION

The purpose of this work is to solve standard problem No. 2 which was proposed by the National Institute of Standards and Technology. This problem consists of computing demagnetization curves of a defect-free particle of well defined geometry (see Fig. 1) with the external field applied parallel to the [111] direction and of considering the exchange as well as the magnetostatic interaction, without magnetocrystalline anisotropy. No specific material parameters are needed since the particle size is varied in units of the exchange length $l_{\mathrm{ex}}=(2A\mu_0/J_s^2)^{1/2}$ and all fields are given in units of M_s. Yuan and co-workers[1] made calculations that partly govern the specifications of standard problem No. 2 which show similar switching mechanisms and comparable switching fields to the results obtained in this work. In order to compute demagnetizing fields, asymptotic boundary conditions[2] are used.

II. MODEL AND SIMULATION METHOD

To study the evolution of the system in time we use the Gilbert equation

$$\frac{d\mathbf{J}}{dt}=-|\gamma|\mu_0\mathbf{J}\times\mathbf{H}+\frac{\alpha}{J_s}\mathbf{J}\times\frac{d\mathbf{J}}{dt}, \tag{1}$$

where $\mathbf{J}$ denotes the magnetic polarization with constant magnitude $\mathbf{J}_s$ and α is the damping constant which was set to 1.0. The effective field $\mathbf{H}$ is defined as the variational derivative of the free energy and is given by

$$\mathbf{H}=\frac{2A}{J_s^2}\nabla^2\mathbf{J}+\mathbf{H}_d+\mathbf{H}_{\mathrm{ext}}-\frac{\partial w_{\mathrm{an}}}{\partial\mathbf{J}}, \tag{2}$$

where $\mathbf{H}_d$ is the demagnetizing field which can be deduced from a scalar potential ϕ by $\mathbf{H}_d=-\nabla\phi$ and $\mathbf{H}_{\mathrm{ex}}$ denotes the external field. In this work the magnetocrystalline anisotropy energy density w_{an} was set to zero according to specifications of μMAG standard problem No. 2. To discretize the Gilbert equation we used Galerkin's method which consists of multiplying the equation under consideration by test functions $\varphi_i(\mathbf{r})$ and integrating it over the underlying volume. Each of the test functions is associated with a node i at $\mathbf{r}_i$ such that $\varphi_i(\mathbf{r}_j)=\delta_{ij}$. The extent of all the nodes spans the finite element mesh which in this work was divided into cubic elements. Approximation of the unknown quantities (polarization $\mathbf{J}$ and scalar potential ϕ) is made using linear combinations of the test functions. Those used for approximating the scalar potential are of higher order than those used for the polarization $\mathbf{J}$ in order to avoid a loss of accuracy resulting from different orders of differentiation ($\Delta\phi=\nabla\mathbf{M}$).[3] The Galerkin method finally leads to a system of nonlinear equations for each time step which is solved iteratively by means of the Newton–Rapshon method. Due to the use of asymptotic boundary conditions (ABCs),[4] in order to compute demagnetizing fields a fully implicit method for time integration can be used which is stable even for large time steps.[5] The disadvantage of using ABCs is the fact that elements are needed outside the region of interest. This partly compensates the reduced computation time due to the use of large time steps. In order to find out when the system has reached the equilibrium state the maximum change of the polarization per unit time is checked every time step. In this work the system is said to be in the equilibrium state when this quantity which is proportional to the

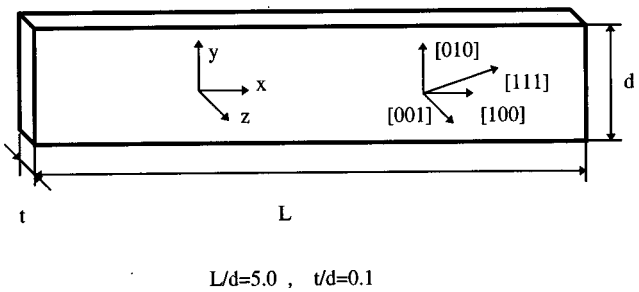

FIG. 1. Particle configuration of μMAG standard problem No. 2. For the calculations in this article the external field is applied parallel to the [100] or parallel to the [111] direction.

 © 1999 American Institute of Physics
[This article is copyrighted as indicated in the article. Reuse of AIP content is subject to the terms at: http://scitation.aip.org/termsconditions. Downloaded to] IP: 142.150.190.39 On: Mon, 22 Dec 2014 09:55:03

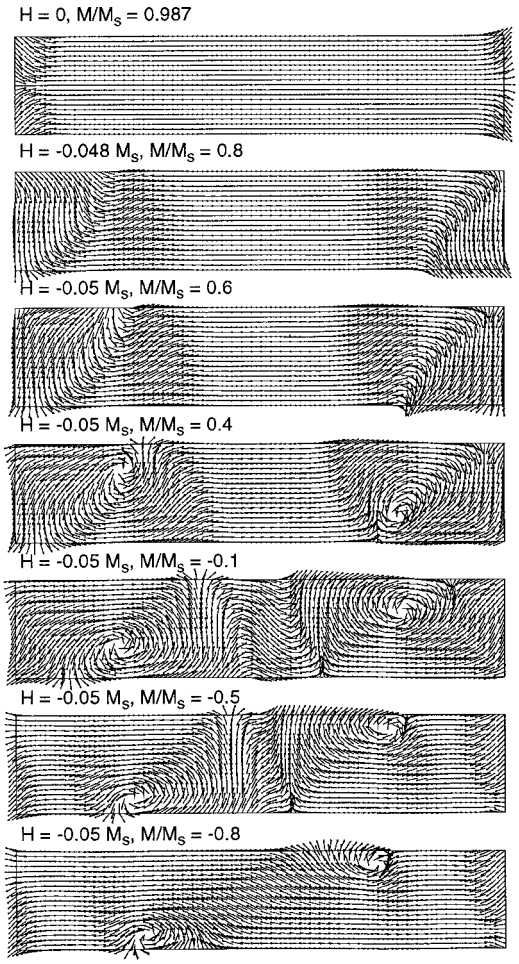

FIG. 2. Remanent and transient magnetic states during irreversible switching of a particle with $d=30\,l_{\mathrm{ex}}$ for an applied field parallel to the [100] axis. The arrows indicate the direction of the magnetic polarization.

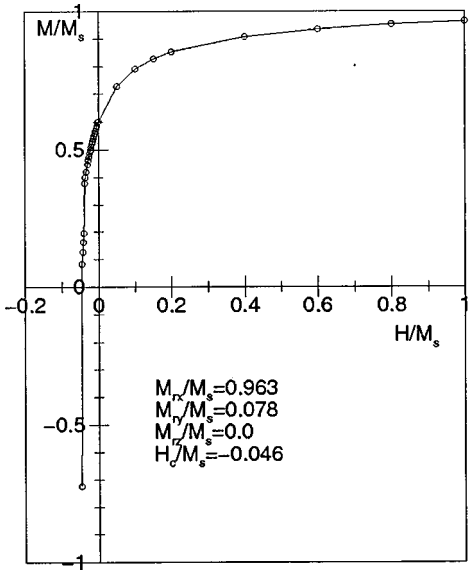

FIG. 3. Demagnetization curve of a particle with $d=30\,l_{\mathrm{ex}}$ for the external field applied parallel to the [111] direction. The circles denote the field values at which the equilibrium states where calculated using the Gilbert equation. The numbers given are the net magetizations in the remanent state and the coercivity.

torque exerted on the polarization vectors falls below $10^{-3}\,J_s^2|\gamma|$ or when the energy starts increasing due to numerical errors. In the latter case the continuation of time integration makes no sense because the energy must necessarily fall when approaching the equilibrium state. For discretization of the geometry of standard problem No. 2 (see Fig. 1) 500 elements were used, 10 along width d, 50 along length L, and one along thickness t of the particle. It is found[6] that for hard magnetic particles a discretization of two nodes per exchange length l_{ex} is enough to properly obtain the coercivities. However, numerical experiments showed that the coercive field $|H_c|$ of well discretized particles (more than two nodes per exchange length l_{ex}) with zero magnetocrystalline anisotropy still increases with increasing mesh density. This effect may be attributed to an underestimation of the exchange energy which dominates in particles with zero magnetocrystalline anisotropy. Therefore the coercivities $|H_c|$ obtained from the simulations must be interpreted as lower limits, especially for the biggest particles considered, those with widths $d=30\,l_{\mathrm{ex}}$.

III. RESULTS

The above algorithm was applied to calculate the magnetization reversal of the particle configuration given in Fig. 1 with the applied field parallel to either the [100] or the [111] direction. The size of the particle was varied from $d=l_{\mathrm{ex}}$ to $d=30\,l_{\mathrm{ex}}$ while keeping the length ratios unchanged. The demagnetization curves were calculated quasistatically with a fully saturated polarization configuration as the initial condition. Starting from $H_{\mathrm{ext}}=M_s$ the field was reduced in steps of $0.2\,M_s$, $0.05\,M_s$, and $0.002\,M_s$ for the external field in intervals [1.0–0.2], [0.2–0.0], and $[0.0\,H_c]$, respectively. The external field decreased after an equilibrium state, defined in Sec. II, was reached.

TABLE I. Observed net magnetizations in the remanent state and coercivities for varying particle extensions. The external field is either parallel to the [100] or the [111] direction.

$H_{\mathrm{ext}}^{\parallel}$	111				100			
d/l_{ex}	M_x/M_s	M_y/M_s	M_z/M_s	H_c/M_s	M_x/M_s	M_y/M_s	M_z/M_s	H_c/M_s
1	0.999	0.029	−0.004	−0.056	0.999	0.001	0.000	−0.380
5	0.999	0.006	0.000	−0.056	0.999	0.001	0.000	−0.148
10	0.998	0.020	0.000	−0.054	0.999	0.001	0.000	−0.078
20	0.973	0.081	0.000	−0.050	0.996	0.000	0.000	−0.056
30	0.963	0.078	0.000	−0.046	0.987	0.000	0.000	−0.048

[This article is copyrighted as indicated in the article. Reuse of AIP content is subject to the terms at: http://scitation.aip.org/termsconditions. Downloaded to] IP: 142.150.190.39 On: Mon, 22 Dec 2014 09:55:03

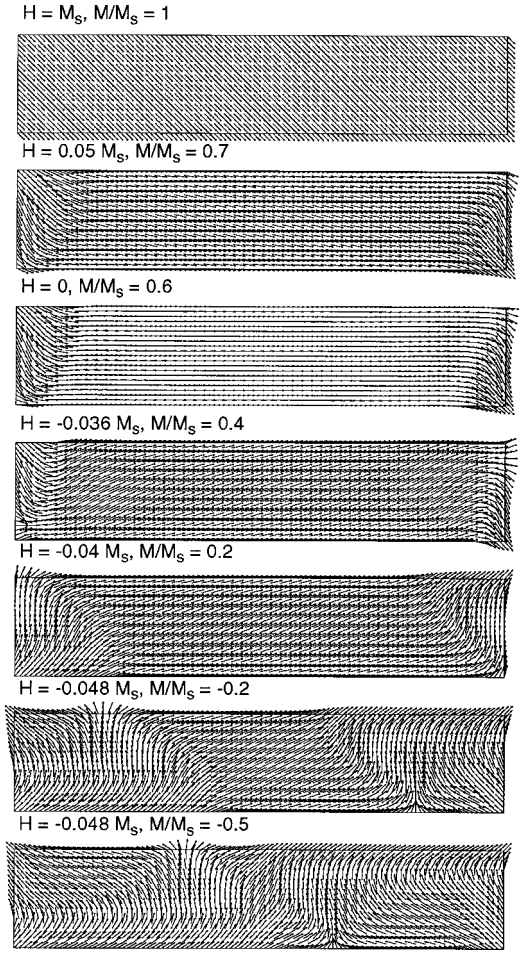

FIG. 4. Magnetization distributions for different M/M_s along the demagnetization curve.

Figure 2 gives the remanent and transient magnetic states during irreversible switching of a particle with $d=30\,l_{\mathrm{ex}}$ at an applied field, $H_{\mathrm{ext}}=-0.048\,M_s$, parallel to the [100] axis. For zero applied field a magnetic flower state is observed. At an applied field of $H_{\mathrm{ext}}=-0.03\,M_s$ the flower state vanishes and end domains form. As a consequence, the net magnetization is reduced from 0.98 to $0.8\,M_s$. The end domains further develop into vortices that head towards each other and lead to an increase of exchange energy and magnetostatic energy. When the final (closed) vortices are formed, flux closure causes a dramatic decrease in the demagnetizing energy. In what follows the regions of the vortices with magnetization parallel to the field direction enlarge. Thus the vortices expand in the direction of the long axis and the centers of the vortices move to opposite sides of their original position as can be seen in Fig. 2. The vortices move further towards each other and thus cause an increase in the magnetic volume and surface charge density, leading to an increase in the magnetostatic energy. When this strongly inhomogeneous magnetic state becomes uniform, the magnetostatic and exchange energies decrease rapidly.

Figure 3 gives the calculated demagnetization curve of a particle with $d=30\,l_{\mathrm{ex}}$ when the external field is applied parallel to the [111] direction. The magnetization distributions given in Fig. 4 clearly show the transition from a uniform magnetic state with the magnetization parallel to the external field to a nearly uniform state with the magnetization parallel to the long axis as the external field is reduced to zero. A component of the external field parallel to the short axis of the particle supports the formation of end domains, which are not observed in the remanent state for H_{ext} parallel to [100]. This difference in remanent states which has yet to be investigated may be attributable to either too loose a criterion for equilibrium for the calculations with H_{ext} parallel to [100] or to the history of the applied field. When the external field becomes negative, the magnetization rotates uniformly within the center of the particle whereas the end domains remain stable up to an external field of $H_{\mathrm{ext}}=-0.038\,M_s$. At this critical external field value the demagnetization curve shows a steep decrease that is associated with the sudden reversal of the end domains towards the applied field direction. This step in the demagnetization curve is only observed for particles with $d\geqslant 20\,l_{\mathrm{ex}}$ whereas for smaller particles no end domains occur in the remanent state.

Table I summarizes the numerical results obtained for the field applied in the [100] direction and the field applied in the [111] direction (μMAG standard problem No. 2). Whereas a significant coercive field size dependence was found for H_{ext} parallel to [100], H_c remains nearly constant as a function of particle size for H_{ext} parallel to [111]. The numerical studies show that the magnetization reversal mechanism changes from a uniform rotation overhead to a head domain wall motion[7] to a vortex motion[1] when the field is applied parallel to the [100] direction. As described above, magnetization reversal is mainly governed by uniform rotation when the field is applied parallel to the [111] direction. The end domains formed in particles with $d\geqslant 20\,l_{\mathrm{ex}}$ cause a step in the demagnetization curve, but do not influence the coercive field.

[1] S. Yuan, H. Bertram, J. Smyth, and S. Schultz, IEEE Trans. Magn. **28**, 3171 (1992).
[2] B. Yang and D. R. Fredkin, J. Appl. Phys. **79**, 5755 (1996).
[3] T. Schrefl, J. Fidler, K. J. Kirk, and J. N. Chapman, J. Magn. Magn. Mater. **175**, 193 (1997).
[4] A. Khebir, A. Kouki, and R. Mittra, IEEE Trans. Microwave Theory Tech. **38**, 1427 (1990).
[5] Y. Nakatani, Y. Uesaka, and N. Hayashi, Jpn. J. Appl. Phys., Part 1 **28**, 2485 (1989).
[6] W. Rave, K. Ramstöck, and A. Hubert, J. Magn. Magn. Mater. **183**, 329 (1998).
[7] R. McMichael and M. J. Donahue, IEEE Trans. Magn. **32**, 4167 (1997).

[This article is copyrighted as indicated in the article. Reuse of AIP content is subject to the terms at: http://scitation.aip.org/termsconditions. Downloaded to] IP: 142.150.190.39 On: Mon, 22 Dec 2014 09:55:03